Journal of Fluorescence (2019) 29:241–253
https://doi.org/10.1007/s10895-018-2333-1

ORIGINAL ARTICLE

Molecular and NLO Properties of Red Fluorescent Coumarins – DFT Computations Using Long-Range Separated and Conventional Functionals

Nagaiyan Sekar[1] · Santosh Katariya[1] · Lydia Rhyman[2,3] · Ibrahim A. Alswaidan[4] · Ponnadurai Ramasami[2,3]

Received: 18 September 2018 / Accepted: 10 December 2018 / Published online: 15 December 2018
© Springer Science+Business Media, LLC, part of Springer Nature 2018

Abstract

Comparative study of nonlinear optical properties of red fluorescent coumarins was carried out with density functional theory based ab initio method using the popular global hybrid (GH) and range separated hybrid (RSH) functionals and correlated with the spectroscopic values. The GHs - M06 L, PBE1PBE, M06, BHHLYP, M062X and M06HF and RSHs - HISSbPBE, wB97, wB97X, HSEH1PBE, CAM-B3LYP and wB97XD in combination with the double zeta basis function 6–311 + G(d,p) were used. The computed polarizability (α_0), hyperpolarizability of the first order (β_0) and second order (γ) computed by the RSHs are closer to the spectroscopic values compared to GHs. Polarizabilities computed with the functionals BHHLYP and M06-2X are closer with the spectroscopic values. Incorporation of additional cyano group enhances the NLO response. An increase in electrophilic nature contributed from the reduced orbital band gap culminating an increase in α_0, β_0, and γ in all the cases. The NLO response was found to be highly solvent dependent that is the polarity of the micro environment created by the solvents. To understand the agreement and accuracy among the NLO parameters obtained from the selected DFT functionals and the spectroscopic values, the mean absolute error (MAE) and vibrational contribution parameters are presented. Two photon absorption (TPA) cross section depends upon the molecular structure where π-framework is an important factor rather than number of acceptors.

Keywords Red fluorescent coumarins · DFT · Nonlinear optical properties · GHs and RSHs

Introduction

Organic compounds having reasonably high nonlinear optical (NLO) properties are mostly desirable as against those of inorganic origin [1–3]. NLOphoric organic molecules with push-pull or Donor-π-Acceptor (D-π-A) configurations studied are mainly from porphyrins [4, 5], phthalocyanines [6–8], azo dyes [9, 10], coumarins [11, 12], styryl dyes [13] and in recent years BODIPY dyes [14–17]. Computing NLO properties using DFT and comparing with spectroscopically derived parameters is an active subject of investigation [18–20]. Though the popular density functional theory (DFT) and time-dependent density functional theory (TD-DFT) based ab initio methods are useful tools in computing the molecular properties of organic molecules, the charge transfer (CT) aspects of the molecules are not reliably computationally assessed using the standard functionals and they give considerable errors [21–23]. The errors originate from the incorrect long-range form of the exchange potential associated with density functionals. There are attempts to circumvent the errors using hybrid functionals [24] as they comprise of some exact exchange modifying the long-range form of the functional [25–27]. The most commonly used GGA and traditional hybrid functionals higher than the expected values of the properties associated with the excited states needed particularly in evaluating the NLO properties [28–32] of molecules associated with an asymmetric, low-lying, and long-range CT

Electronic supplementary material The online version of this article (https://doi.org/10.1007/s10895-018-2333-1) contains supplementary material, which is available to authorized users.

✉ Nagaiyan Sekar
n.sekar@ictmumbai.edu.in; nethi.sekar@gmail.com

✉ Ponnadurai Ramasami
p.ramasami@uom.ac.mu; ramchemi@intnet.mu

[1] Department of Dyestuff Technology, Institute of Chemical Technology, Nathalal Parekh Marg, Matunga, Mumbai 400 019, India

[2] Computational Chemistry Group, Department of Chemistry, Faculty of Science, University of Mauritius, Réduit 80832, Mauritius

[3] Department of Applied Chemistry, University of Johannesburg, Doornfontein Campus, Johannesburg 2028, South Africa

[4] Department of Pharmaceutical Chemistry, College of Pharmacy, King Saud University, Riyadh 11451, Saudi Arabia

resonance state, and such molecules invariably possesses large bulk NLO properties [33–35]. On considering the computational cost and accuracy, it is demonstrated that long-range corrected (LC) DFT could be reliable for computing the hyperpolarizabilities [36–42]. The success of LC-DFT in describing acceptable excited state phenomena is attributed to the required fraction of Hartree-Fock exchange incorporated with increasing inter-electronic distance [43–53]. The range separated hybrid (RSH) functionals used in LC-DFT are constructed by separating the exchange energy, E_X in short and long-range (SR and LR) contributions,

$$E_X^{LC-DFT} = E_X^{SR-DFT} + E_X^{LR-HF} \quad (1)$$

which is achieved by bifurcating the interelectronic Coulomb operator r_{12}^{-1}

$$\frac{1}{r_{12}} = \underbrace{\frac{1-erf(\omega r_{12})}{r_{12}}}_{SR} + \underbrace{\frac{erf(\omega r_{12})}{r_{12}}}_{LR} \quad (2)$$

with erf defined as the inaccuracy function and ω as the parameter describing the range separation.

Molecular materials undergoing facile singlet fission (SF) have enhanced NLO properties [54]. The most important requirement for an effective SF is based on the energy criterion in organic molecules, given by Eq. (3) [55],

$$E_{SF} = E_{S1} - 2 \times E_{T1} \approx 0 \quad (3)$$

where E_{T1} is the difference in energy between the ground and first triplet excited state which is approximately half the energy needed for excitation to the first singlet excited state, E_{S1}. Thus singlet-triplet distribution in the virtual orbitals of a molecule helps in understanding the NLO properties of organic molecules.

In view of the above and importance of NLOphoric molecules, this paper focuses on the evaluation of the suitability of GH functionals with that of RSH functionals for the computation of total polarizability (α_0), the static first and second order hyperpolarizabilities β_0 and γ_0 of red fluorescent coumarins. TD-DFT based triplet state population is also studied. The GHs and RSHs utilized as a part of the investigation with their constituent percentage of HF composition are provided in Table 1.

The present investigation should encourage the proposal of different molecules with large desired degree of linear and NLO reaction in functional organic materials. The molecules considered in this study are given in Fig. 1.

Materials and Methods

All the calculations were performed with Gaussian 09 suit program [56] with the of the computational resources made available by GridChem Science Gateway [57–59] The GH functional B3LYP which employs Becke's three parameter (local, non-local) hybrid exchange functional with Lee–Yang–Parr correlation functional [60] inflated with triple zeta basis set 6–311 + G(d,p) [61, 62] was used in the optimization of the ground state geometry. Time-dependent density functional theory (TD-DFT) [63] at the same level of theory was employed for obtaining vertical excitations. DFT and TD-DFT calculations in solvent environments were performed with the PCM model as implemented in Gaussian 09 [64]. The consolidated polarizability and the values of static first and second order hyperpolarizabilities were calculated using finite field approach [65] as implemented in Gaussian 09 using both GHs and RSHs. The detailed description is given in the eq. S1.

Table 1 GHs and RSHs functionals with their percent HF exchange composition

Global hybrids (GHs)		Range separated hybrids (RSHs)	
Functional	HF %	Functional	HF %
M06 L	0	HISSbPBE	–
PBE0	25	wB97	15
M06	27	wB97X	25
BHHLYP	50	HSEH1PBE	19–65
M06-2X	54	CAM-B3LYP	22–100
M06-HF	100	wB97X-D	.

The GHs used for polar computations are M06 L, PBE1PBE, M06, BHHLYP, M062X, and M06HF while the RSHs used are, HISSbPBE, wB97, wB97X, HSEH1PBE, CAM-B3LYP and wB97XD. The quantum mechanical molecular descriptors - chemical hardness (η), softness (S) and electrophilicity index (ω) were accessed from HOMO and LUMO energies.

The values of total static dipole moment (μ), the mean polarizability (α_0), the anisotropy of the polarizability ($\Delta\alpha$), the mean first hyperpolarizability (β) and static second hyperpolarizability (γ), of the C1-C4 dyes in different solvent environments were calculated using the GHs and RSHs and the Pople's basis set 6–311 + G(d,p) inflated with two polarization functions and one diffuse function using the equations provided in SI.

Result and Discussion

Static Dipole Moment

Ground state static dipole moment (μ) of C1-C4 were calculated in different solvents at the same level of theory. The static dipole moment increases as the polarity of solvent increases, and this trend was observed with all the functionals. The static dipole moment values with all the functionals are in

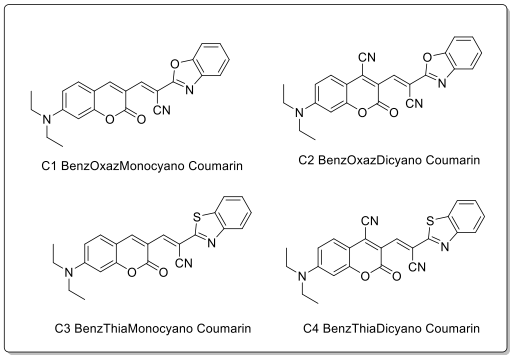

Fig. 1 Structures of C1 to C4 dyes

Structure	Structure
Name	Name
Structure	Structure
Name	Name

the order: **C1 > C3 > C2 > C4**. This indicates there is a definite effect of additional cyano group on the value of static dipole moment. GHs and RSHs give similar values of static dipole moment for the four dyes Table S0. That is the dipole moment values are independent of the functional being used.

We focused on the energies of HOMO and LUMO in order to estimate the molecular properties to ascertain whether correlations exist with chemical stabilities exist. According to Koopmans' theorem, the energy HOMO (E_{HOMO}) is related to the ionization potential (IP) and the energy LUMO (E_{LUMO}) is used to estimate the electron affinity (EA). The chemical stability of a compound relies upon hardness and softness values. We can classify as to whether the chemical nature of the molecule is soft or hard [63, 66] from the HOMO-LUMO energy gap. The molecules with the lower energy band gap lead to more softness and vice versa. The electrophilicity index (ω) which defines electrophilic power - the energy lowering accompanied by the facile flow of electrons between donor and acceptor orbitals - of a molecule is inversely proportional the hardness. From Table 2, Table S1 and Fig.S1, it is observed that the energy band gaps (E_L-E_H) of the molecules are in respectable agreement with ω and the trend is **C1 > C2 and C3 > C4.** The hardness of a molecule can be determined using Eq. (4),

$$\eta = \frac{(-E_{HOMO} + E_{LUMO})}{2} \tag{4}$$

where,

the η = hardness of molecule,

E_{HOMO} and E_{LUMO} indicate respectively the energies associated with the HOMO and LUMO.

Quantum yield values were taken from our earlier work [11].

Singlet-Triplet Distribution

The TD-DFT computations indicate that **C1-C4** have the same disposition of singlets and triplets in their excited states. All the dyes have two triplet states occurring between the ground state S_0 and the first excited singlet state S_1. Usually the triplet state is more stable and lies at a lower energy level in comparison with the singlet state. The energies of the ground state (GS) singlet (S_0), excited state (ES) singlet (S_1) and ES triplet (T_1) are computed with TD-DFT calculations, and the corresponding E_{S1} (the difference energy in energy between S_1 and S_0), E_{T1} (the difference energy between T_1 and S_0) and E_{ISC} (intersystem crossing energy, the difference in energy between S_1 and T_1 states) values were calculated for the dyes and they are recorded in Table 2. The triplet state is closer to S_1. For all the dyes, $2E_{T1} > E_{S1}$, and therefore there are increasing prospects of ISC which is further supported by low E_{ISC} Fig. 2.

Table 2 Energy of HOMO, LUMO, chemical hardness (η), Global softness (S), Electrophilicity index (ω), energy of intercrossing system (E_{ISC}) and fluorescent quantum yield (φ) of the dyes C1 to C4 in methanol

Dye	E_{LUMO} (eV)	E_{HOMO} (eV)	E_L-E_H (eV)	η (eV)	S (eV)	ω (eV)	E_{ISC} (eV)	E_{SF}	φ
C1	−2.96	−5.80	2.84	1.4	0.704	6.75	0.0996	−2.383	0.0157
C2	−3.58	−5.98	2.40	1.2	0.835	9.53	0.0418	−2.132	0.0121
C3	−2.95	−5.77	2.82	1.4	0.708	6.74	0.0896	−2.378	0.0061
C4	−3.56	−5.95	2.39	1.2	0.837	9.46	0.0289	−2.147	0.0157

Quantum yield values are taken from reference [11]

The energy of intersystem crossing E_{ISC} was evaluated in each case and are given in Table 2 together with the magnitudes of their quantum yield values. The value of quantum efficiency of **C3** is lower as compared to **C1**, **C2** and **C4**. Quantum yield is larger in the case where the energy intersystem crossing, E_{ISC} gap is larger [67]. From the distribution pattern of singlet and triplet states, it can be concluded that the dyes with higher quantum yield show better NLO properties.

Polarizability, Hyperpolarizability and Second Order Hyperpolarizability

Polarizability

A knowledge of the NLO behaviors is important in the design of newer molecules for optical memory devices communication technology and optical switches. The strength of optical response depends on the electrical properties of the material that is the polarizability (α, linear response) of compounds.

We estimated the polarizability (Fig. 3, Table S2) of C1-C4 by the solvatochromic method and compared with those calculated. Polarizability increases as the solvent polarity increases, and this trend is seen with all the 12 functionals. The polarizability values obtained from each functional are almost in the order: C4 > C2 > C3 > C1 indicating that additional cyano group increases the polarizability. Polarizabilities computed with the functionals BHHLYP and M06-2X are closer with the spectroscopic values. The computed values of α_0 obtained from the functionals M06, M06HF, PBE1PBE, and M06-L are nearly same. The values

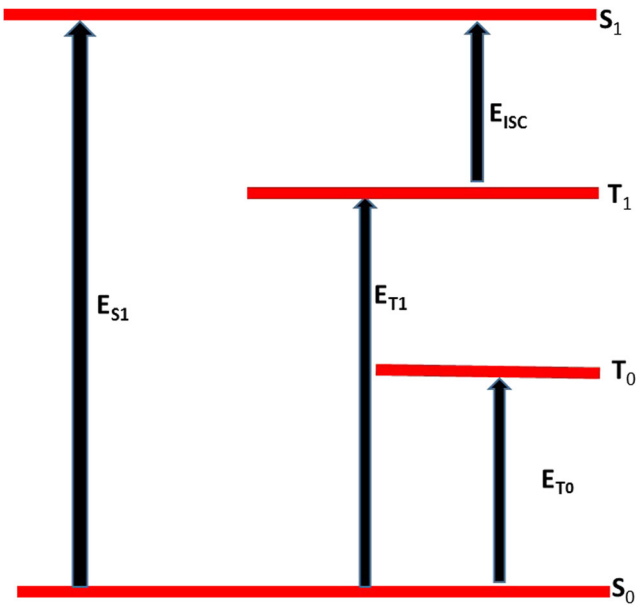

Fig. 2 Singlet-triplet distribution in C1 to C4 dyes

computed with both the functionals, wB97 and wB97X are closer to experimental values. Among the RSHs, the values computed from CAM-B3LYP, wB97XD, HISSbPBE and HSEH1PBE functionals are comparable with each other. The computed values from RSHs are lower than those from GHs. Fig 3 and Table S2.

Hyperpolarizability

Hyperpolarzability of the first order (β) is a measure of the NLO response of materials, and β is associated with the ICT, resulting from the movement of electrons in push-pull systems. Cooperative communication between the electron density with an external electric field influencing the magnitude and direction of the dipole moment as well as second order NLO response. By knowing hyperpolarizabilities of coumarin dyes, it would be interesting and useful to find out the influence of cyano substitution on NLO responses.

We estimated first hyperpolarizability (Fig. 4 and Table S3) of C1-C4 by the solvatochromic method and compared them with the calculated values obtained from (GH) and (RSH) functional. We noticed in all 12 different functionals, hyperpolarizability values increase as the polarity of solvent increases. The polarizabilities in each functional are in the order: C4 > C2 > C3 > C1. This indicates that additional cyano group increases the hyperpolarizability value. Among the GHs, M06, M06HF and BHHLYP functionals show closer values with those obtained experimentally. The values of β_0 computed with the GHs M06, M06HF, and M06-L, PBE1PBE, and M062X are seen to be more or less similar each other in their magnitudes. The values obtained with the HISSbPBE and HSEH1PBE functionals are closer to spectroscopic values. Among the RSHs, the values computed by CAM-B3LYP, wB97XD, wB97and wB97X functionals are comparable with each other. The values obtained with RSHs are larger than those obtained with GHs (Fig. 4 and Table S3).

The product of static dipole moment with mean first hyperpolarizability ($\mu\beta_0$) are summarized in Fig. 5 and Table S4. The $\mu\beta_0$ values are in the order: C4 > C2 > C3 > C1 with almost all the functionals.

First hyperpolarizability of all the four dyes lie in the observed intrinsic range (0.020–0.058); **(**Fig. 6**, Table S5).** The general trend of intrinsic hyperpolarizability is **C4 > C2 > C3 > C1**. This suggests that additional cyano group affects **C4** and **C2** compared to **C1** and **C3. C1** and **C2** have lower values than **C3** and **C4.**

We estimated the second hyperpolarizability (Fig. 7 and Table S6) of C1-C4 by the solvatochromic method and compared them with the calculated values. The hyperpolarizabilities also maintain the same trend as it was

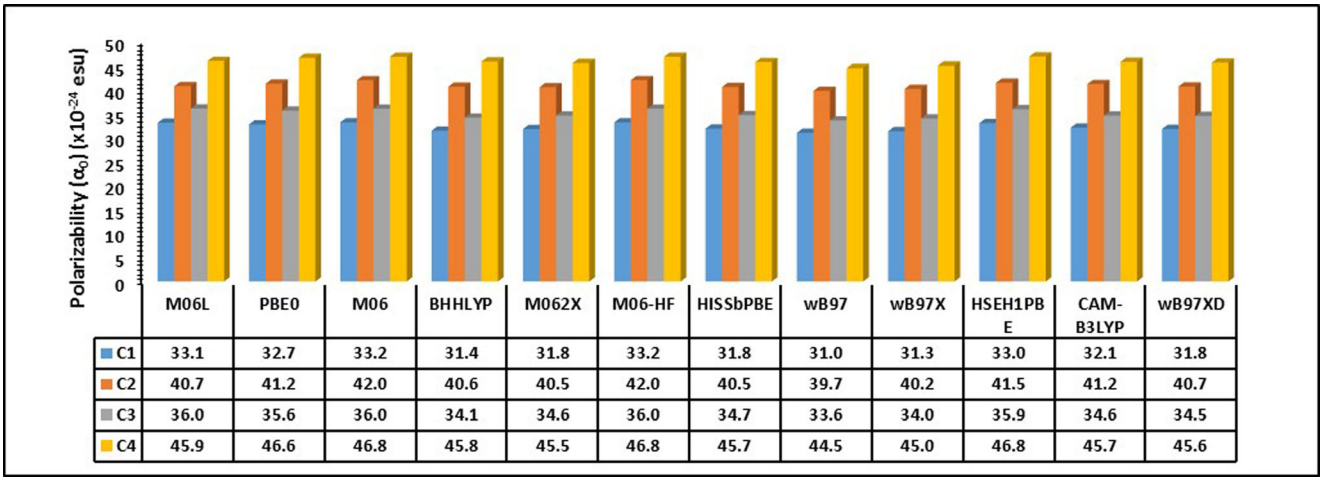

	M06L	PBE0	M06	BHHLYP	M062X	M06-HF	HISSbPBE	wB97	wB97X	HSEH1PBE	CAM-B3LYP	wB97XD
C1	33.1	32.7	33.2	31.4	31.8	33.2	31.8	31.0	31.3	33.0	32.1	31.8
C2	40.7	41.2	42.0	40.6	40.5	42.0	40.5	39.7	40.2	41.5	41.2	40.7
C3	36.0	35.6	36.0	34.1	34.6	36.0	34.7	33.6	34.0	35.9	34.6	34.5
C4	45.9	46.6	46.8	45.8	45.5	46.8	45.7	44.5	45.0	46.8	45.7	45.6

Fig. 3 The linear polarizability ($\alpha_0 \times 10^{-24}$ esu) values with various functionals in ethanol

observed in polarizability and first hyperpolarizability with respect to solvent polarity. The polarizability values in each functional is in the order **C4 > C2 > C3 > C1**. This indicates that additional cyano group increases the second hyperpolarizability values. Among the GHs, BHHLYP shows closer values with those obtained experimentally and the overall order of the functionals is BHHLYP > M062X > M06HF = M06 > PBE1PBE > M06-L. Among the RSHs, the overall order of functionals is wB97 > wB97X > wB97XD > CAM-B3LYP > HISSbPBE > HSEH1PBE. RSHs values are smaller than GHs, Fig. 7 and Table S6.

The comparative outcomes of MAE with respect to all the functionals are provided in Figs. 8, 9 and 10, S2, S3, S4 and Table S7. It is observed that the **C2** and **C4** show greater α_0, β_0, and γ_0 with the substitution of cyano group and reduce the HOMO–LUMO energy gap.

The hyperpolarizabilities of first and second order have significance in molecular systems and they depend on the proficiency of cooperative electronic interaction between donor and acceptor groups. Several researchers have examined the regularity between the spectral shift and computational methods to characterize and design the most competent NLO materials [68–70].

The total polarizability and hyperpolarizabilities computed by GH functionals are comparatively larger than those from RSH functionals. This is anticipated since computations using traditional hybrid functionals are known to result in increased hyperpolarizabilities [71–73]. A number of conceptual [74] and experimental [75] investigations have established this correlation amongst the total hyperpolarizabilities and HOMO – LUMO energy gap (ΔE). The connectivity between these two aspects can be understood in the light of the perseverance of CT interactions, resulting in an increased hyperpolarizabilities, being preferred in molecular structures having lower HOMO–LUMO energy gap (ΔE). **C2** and **C4** have larger polarizability and hyperpolarizability values than **C1** and **C3.**

The dyes **C2** and **C4** containing two cyano groups exhibit the maximum hyperpolarizability values computed using the entire rage of functionals used in this study. This concludes that the substitution pattern of

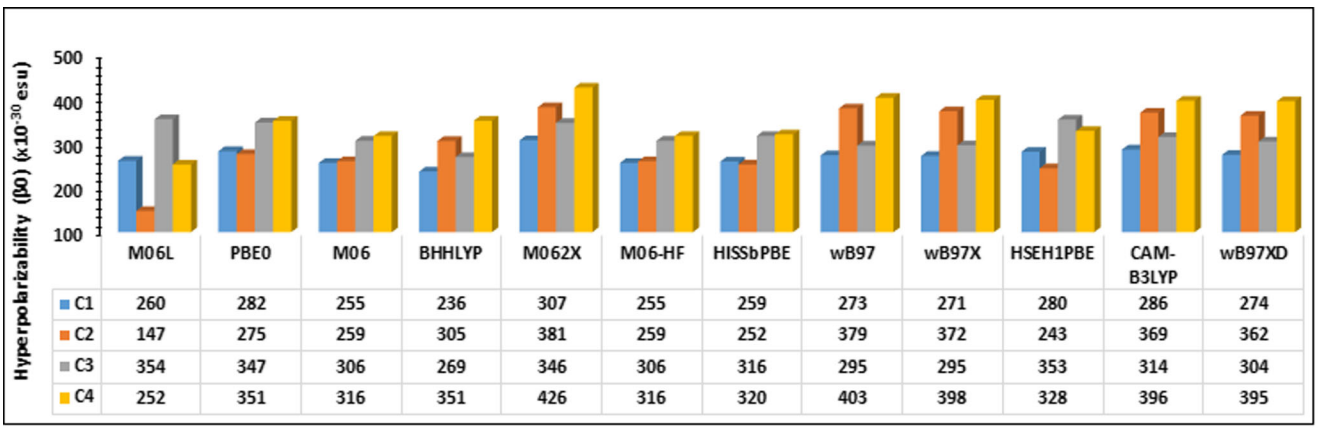

	M06L	PBE0	M06	BHHLYP	M062X	M06-HF	HISSbPBE	wB97	wB97X	HSEH1PBE	CAM-B3LYP	wB97XD
C1	260	282	255	236	307	255	259	273	271	280	286	274
C2	147	275	259	305	381	259	252	379	372	243	369	362
C3	354	347	306	269	346	306	316	295	295	353	314	304
C4	252	351	316	351	426	316	320	403	398	328	396	395

Fig. 4 The first hyperpolarizability ($\beta_0 \times 10^{-30}$ esu) values with various functionals in ethanol

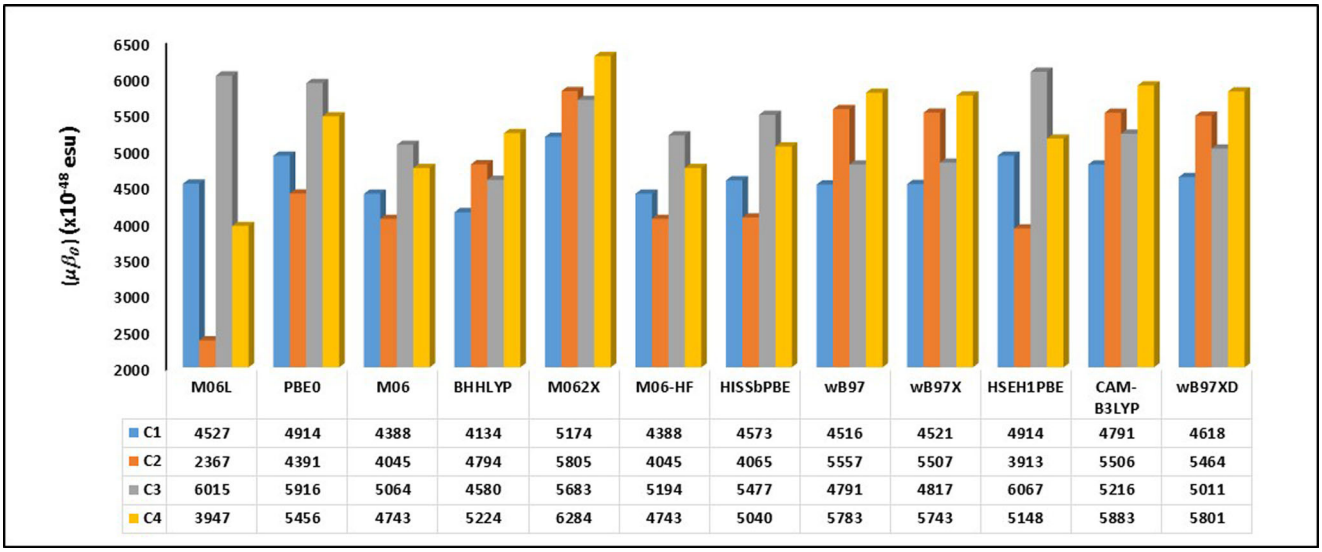

	M06L	PBE0	M06	BHHLYP	M062X	M06-HF	HISSbPBE	wB97	wB97X	HSEH1PBE	CAM-B3LYP	wB97XD
C1	4527	4914	4388	4134	5174	4388	4573	4516	4521	4914	4791	4618
C2	2367	4391	4045	4794	5805	4045	4065	5557	5507	3913	5506	5464
C3	6015	5916	5064	4580	5683	5194	5477	4791	4817	6067	5216	5011
C4	3947	5456	4743	5224	6284	4743	5040	5783	5743	5148	5883	5801

Fig. 5 The $\mu\beta_0$ (× 10^{-48} esu) values for all dyes in ethanol

electron acceptor groups directly affects the extent of polarizability and hyperpolarizability values.

The GH and RSH functionals give some inaccuracies in calculating the polarizability (α_0) and hyperpolarizability values (β_0, γ_0) of the coumarin chromophores under examination. The positive values of MAE signify that they tend to compute higher magnitude for α_0 and β_0, γ_0 values. The trends observed in MAE in different functionals are provided in Figs. 8, 9 and 10, Fig. S2, S3 S4 and Table S7. The MAE values of α_0, β_0 and γ_0 obtained using from the GH functionals are in the range of 3.2–5.6 and 2.3–5.5, 12–54 and 9–58, 95–293 and 90–276 respectively, and that of RSH functionals are towards reasonably lower side. These suggest that the GH functionals might be computing higher the polarizability and hyperpolarizability values. The magnitudes of polarizability and hyperpolarizability are lower in the non-polar solvent environment. The solvatochromic values of α_0, β_0 and γ_0 of **C1 to C4** were taken from reference [76]. The computed values of α_0, β_0, and γ_0 of the C1-C4 examined here are several times higher in magnitude than those of urea [77].

Vibrational Involvement in the Linear and NLO Response

In push-pull systems, vibrational modes are usually intensely coupled with resonating π-electrons in the compound. Hence in determining the NLO properties along with the electronic transitions, the vibrational transitions

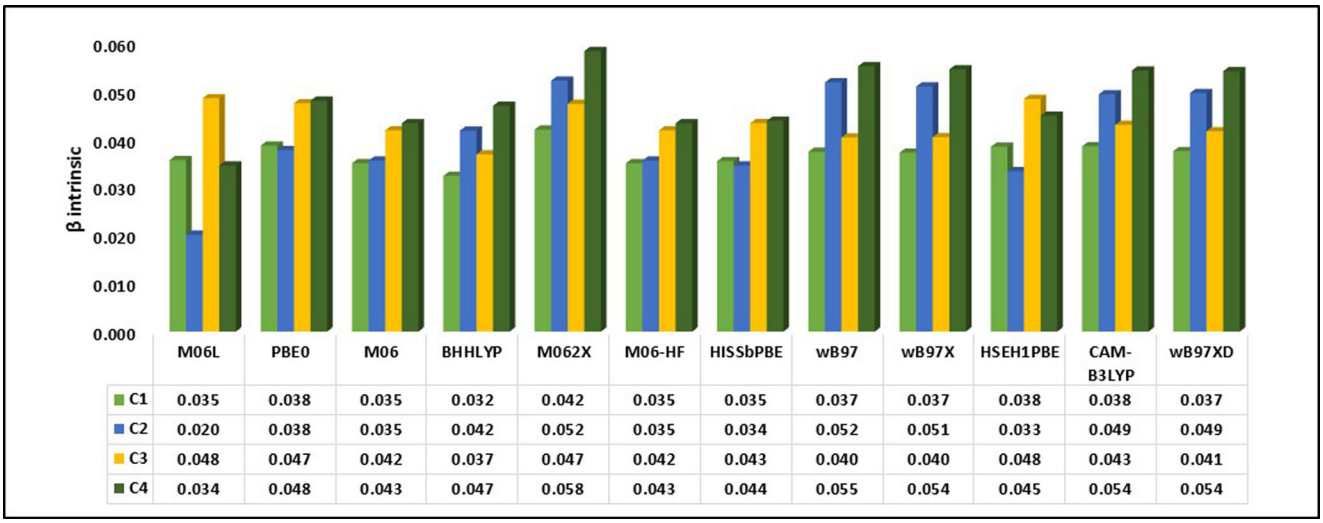

	M06L	PBE0	M06	BHHLYP	M062X	M06-HF	HISSbPBE	wB97	wB97X	HSEH1PBE	CAM-B3LYP	wB97XD
C1	0.035	0.038	0.035	0.032	0.042	0.035	0.035	0.037	0.037	0.038	0.038	0.037
C2	0.020	0.038	0.035	0.042	0.052	0.035	0.034	0.052	0.051	0.033	0.049	0.049
C3	0.048	0.047	0.042	0.037	0.047	0.042	0.043	0.040	0.040	0.048	0.043	0.041
C4	0.034	0.048	0.043	0.047	0.058	0.043	0.044	0.055	0.054	0.045	0.054	0.054

Fig. 6 The intrinsic first hyperpolarizability values for all dyes in ethanol

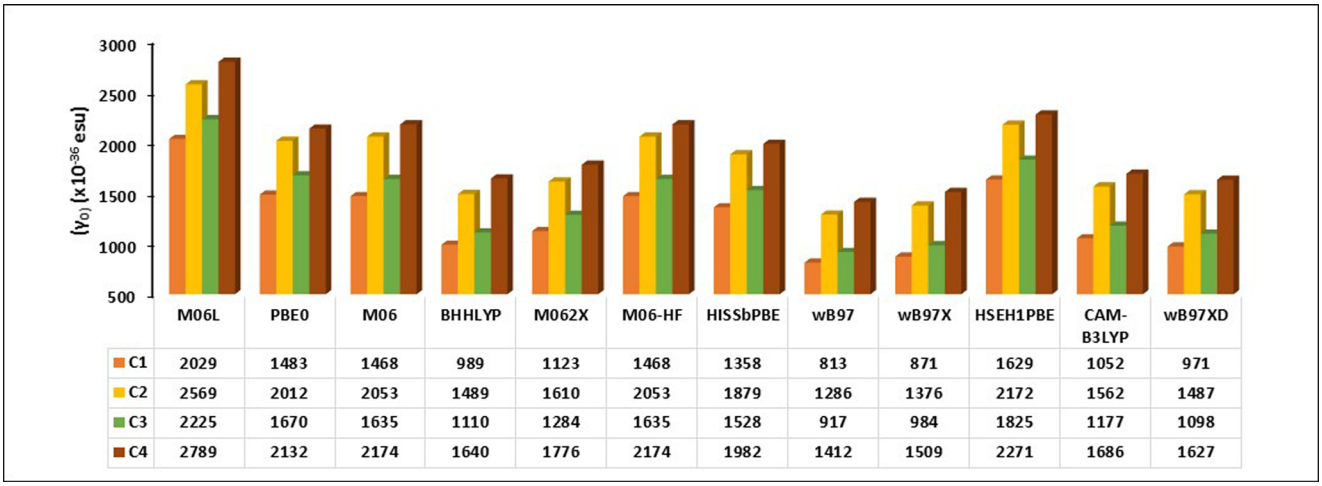

	M06L	PBE0	M06	BHHLYP	M062X	M06-HF	HISSbPBE	wB97	wB97X	HSEH1PBE	CAM-B3LYP	wB97XD
C1	2029	1483	1468	989	1123	1468	1358	813	871	1629	1052	971
C2	2569	2012	2053	1489	1610	2053	1879	1286	1376	2172	1562	1487
C3	2225	1670	1635	1110	1284	1635	1528	917	984	1825	1177	1098
C4	2789	2132	2174	1640	1776	2174	1982	1412	1509	2271	1686	1627

Fig. 7 The second hyperpolarizability (γ) (**$\gamma_0 \times 10^{-36}$ esu**) values for all dyes in ethanol

need to be considered. The cooperative interaction between the electronic polarization arising from delocalization and vibrational transitions result in a large vibrational influence to the total NLO response [78]. In such an instance, DFT is a preferred calculation means to investigate the vibrational impact on the polarizability and hyperpolarizabilities of NLOphoric molecules [79, 80]. We evaluated the vibrational influences to static electronic polarizabilities and hyperpolarizabilities using the method B3LYP/6–311 + G(d,p) in two solvents. Table 3 and S8, S9, S10, S11 present the outcomes of the diagonal electronic and vibrational influences to the linear polarizability (α) and hyperpolarizability of the first order (β). Table 3 shows that in addition to the electronic measure there is the sizeable involvement of the vibrational measure to the polarizability and hyperpolarizability. The ratios of vibrational to electronic contribution in polarizability (α^v/α^e) are 0.226 to 0.296 for C1, 0.293 to 0.368 for C2, 0.224 to0.290 for C3, and 0.296 to 0.373 for C4 in toluene (non-polar) and methanol (polar with hydrogen bonding capabilities) respectively. In case of hyperpolarizabilities of the first order, the ratios of vibrational to electronic contribution (β^v/β^e for C1–0.887 to −0.822, C2–0.794 to −0.685,C3–0.709 to −0.710 and C4–0.610 to-0.595 Table 3 are in toluene and methanol respectively. This endorses the fact that the vibrational motions have an important role to play in contributing to the NLO

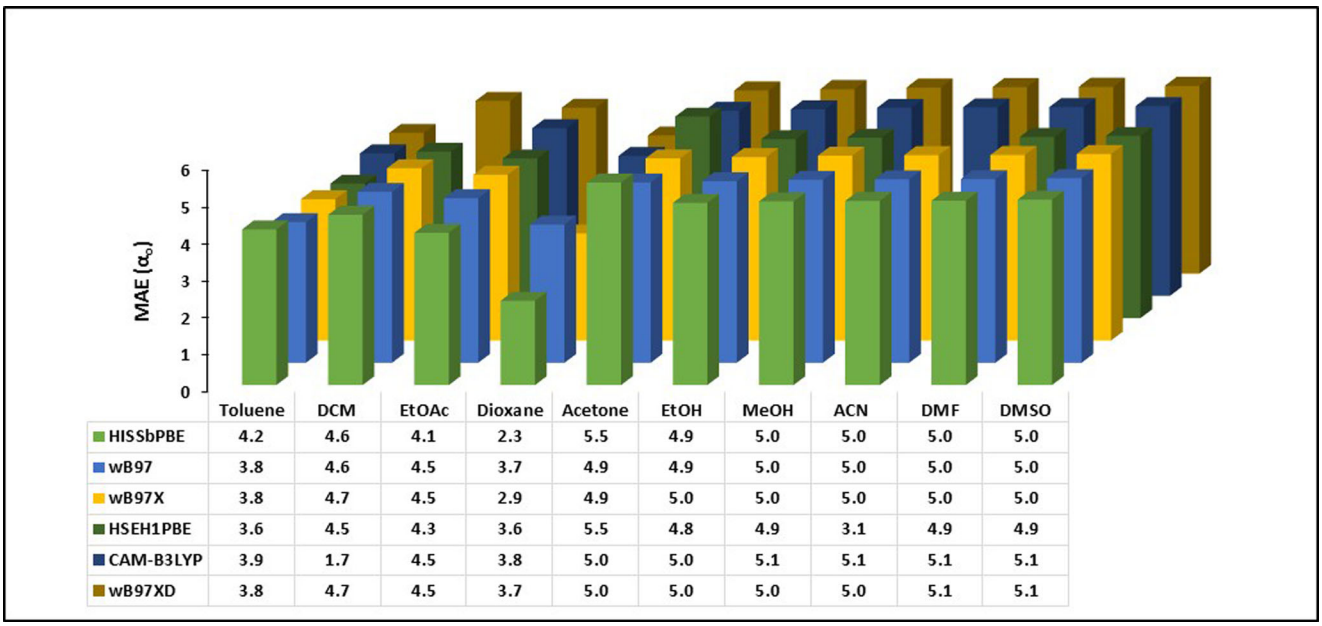

	Toluene	DCM	EtOAc	Dioxane	Acetone	EtOH	MeOH	ACN	DMF	DMSO
HISSbPBE	4.2	4.6	4.1	2.3	5.5	4.9	5.0	5.0	5.0	5.0
wB97	3.8	4.6	4.5	3.7	4.9	4.9	5.0	5.0	5.0	5.0
wB97X	3.8	4.7	4.5	2.9	4.9	5.0	5.0	5.0	5.0	5.0
HSEH1PBE	3.6	4.5	4.3	3.6	5.5	4.8	4.9	3.1	4.9	4.9
CAM-B3LYP	3.9	1.7	4.5	3.8	5.0	5.0	5.1	5.1	5.1	5.1
wB97XD	3.8	4.7	4.5	3.7	5.0	5.0	5.0	5.0	5.1	5.1

Fig. 8 Polarizability ($\alpha_0 \times 10^{-24}$ esu) MAE from RSHs

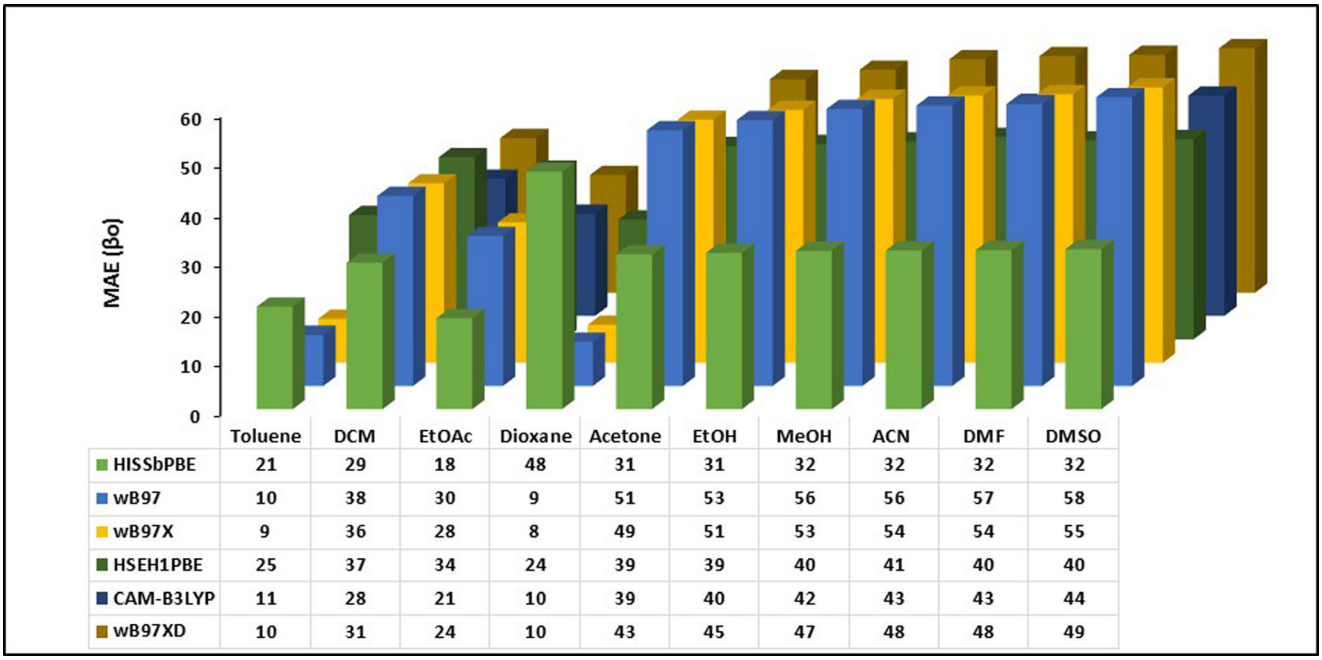

	Toluene	DCM	EtOAc	Dioxane	Acetone	EtOH	MeOH	ACN	DMF	DMSO
HISSbPBE	21	29	18	48	31	31	32	32	32	32
wB97	10	38	30	9	51	53	56	56	57	58
wB97X	9	36	28	8	49	51	53	54	54	55
HSEH1PBE	25	37	34	24	39	39	40	41	40	40
CAM-B3LYP	11	28	21	10	39	40	42	43	43	44
wB97XD	10	31	24	10	43	45	47	48	48	49

Fig. 9 The first hyperpolarizability ($\beta_0 \times 10^{-30}$ esu) MAE from RSHs

properties of C1-C4, especially in polar surroundings wherein solvation has a decisive influence in vibrations.

Limits for the First and Second Order Hyperpolarizability Values

For **C1** to **C4** push-pull chromophores the fundamental limits of NLO descriptors can be estimated using the limiting theory proposed by Kuzyk [81, 82]. It is the sum-rule-restricted (SR) three-level model which produces a two-level-limit (2 L) for β (β_{2L}^{*SR} or βmax) which is entirely dependent on the π electrons (N) in conjugation from double or triple bond and the transition energy E_{10} between the ground and first excited states, deduced from steady state absorption spectra. The limit is calculated using Eq. (5) in different solvents with the help of their respective refractive indices (n) of the solvent.

$$\beta_{2L}^{*SR} \leq \sqrt[4]{3}\left(\frac{n^2+2}{3}\right)^3\left(\frac{e\hbar}{\sqrt{m}}\right)^3\frac{N^{\frac{3}{2}}}{E_{10}^{\frac{7}{2}}} \tag{5}$$

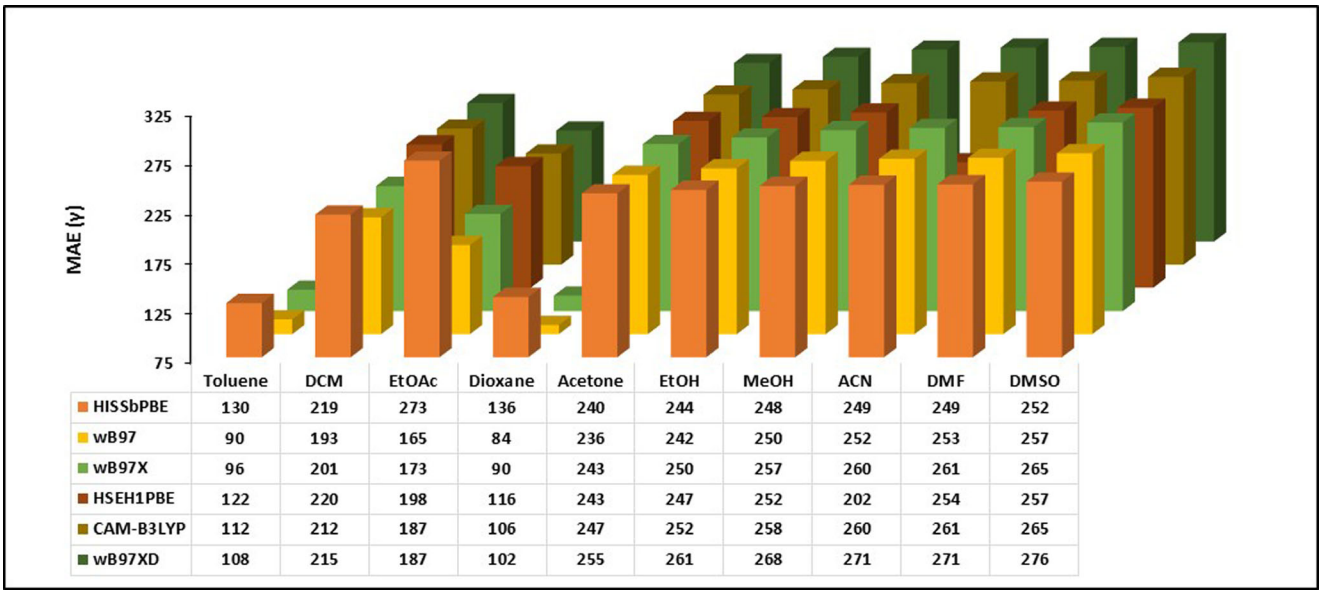

	Toluene	DCM	EtOAc	Dioxane	Acetone	EtOH	MeOH	ACN	DMF	DMSO
HISSbPBE	130	219	273	136	240	244	248	249	249	252
wB97	90	193	165	84	236	242	250	252	253	257
wB97X	96	201	173	90	243	250	257	260	261	265
HSEH1PBE	122	220	198	116	243	247	252	202	254	257
CAM-B3LYP	112	212	187	106	247	252	258	260	261	265
wB97XD	108	215	187	102	255	261	268	271	271	276

Fig. 10 The second hyperpolarizability ($\gamma_0 \times 10^{-36}$ esu) MAE from RSHs

Table 3 Diagonal electronic and vibrational contributions to dipole polarizabilities and first hyperpolarizabilities of dyes C1 to C4 obtained from of B3LYP/6–311 + G(d,p) level in toluene and ethanol medium

Dye	C1		C2		C3		C4	
Property	Toluene	EtOH	Toluene	EtOH	Toluene	EtOH	Toluene	EtOH
α_{xx}^{e}	942	1120.7	1040	1287.7	972	1159.8	1066	1328.1
α_{yy}^{e}	38	55.1	−41	−62.1	34	53.2	−38	−65.7
α_{zz}^{e}	354	429.8	387	474.3	390	479.2	420	524.2
α_{xx}^{v}	180	300.7	178	320.6	186	312.8	186	336.4
α_{yy}^{v}	50	74.4	68	90.6	50	77.9	73	105.8
α_{zz}^{v}	71	100.6	161	214.5	77	113.4	171	225.5
α^{e}	445	535.2	462	566.633	465	564.067	483	595.533
α^{v}	101	158.567	136	208.567	104	168.033	143	222.567
$\alpha^{e} + \alpha^{v}$	545	693.767	598	775.2	569	732.1	626	818.1
α^{v}/α^{e}	0.2262	0.29628	0.2934	0.36808	0.2245	0.2979	0.2963	0.37373
β_{xxx}^{e}	17831	34026.9	12736	30866.3	22724	41898.5	18,713	−40312
β_{yyy}^{e}	−608	−1994.9	2594	5936.9	−162	−1018	1462	−3673.6
β_{zzz}^{e}	−857	−1468.8	−1304	−2594.4	−868	−1546.4	−1388	2878.6
β_{xzx}^{v}	−13179	−22884	−12427	−25076	−13543	−24681.6	−12797	26460.2
β_{yyy}^{v}	−1111	−1642.2	974	1332.1	−1319	−2109.1	1454	−2407.1
β_{zzz}^{v}	−231	−602.7	307	310.2	−538	−1153.3	−135	443.4
β^{e}	5455	10187.7	4675	11402.9	7231	13111.4	6262	−13702
β^{v}	−4840	−8376.3	−3715	−7811.3	−5133	−9314.67	−3826	8165.5
$\beta^{e} + \beta^{v}$	615	1811.47	960	3591.63	2098	3796.7	2436	−5536.7
β^{v}/β^{e}	−0.8872	−0.8222	−0.7946	−0.685	−0.7098	−0.71043	−0.6109	−0.5959

(All values are in a.u)

e and m are the charge and mass of the electron, and $\hbar = h/2\pi$.

Likewise, the limit for the second order hyperpolarizability (γ) can be estimated by eq. (6) [83, 84]. The values of γ have usually two conceivable essential limits for the i.e. negative limit which is for a centro symmetric molecule and positive limit for a non-centrosymmetric molecule.

$$-\frac{e^4\hbar^4}{m^2}\left(\frac{N^2}{E_{10}^5}\right) \leq \gamma \leq 4\frac{e^4\hbar^4}{m^2}\left(\frac{N^2}{E_{10}^5}\right) \quad (6)$$

The limiting values for β and γ calculated with the help of Eqs. (5) and (6) are compared with the corresponding values obtained by spectroscopic and computational approaches for **C1** to **C4** in Table 4 and Table S12.

Two-Photon Absorption Cross Section

Two-photon absorption (TPA) is a distinctive nonlinear optical attribute of a largely π-delocalized system with an impending CT features [85]. On the basis of linear spectroscopic measurements, the variation in dipole moment, the molar absorptivity and the frequency of the absorption maximum of the one-photon absorption band, the TPA cross sections are described within the ambit of a two-level approximation [86, 87] by using Eq. (7).

Table 4 Comparison of solvatochromic and theoretical values with the limiting values of hyperpolarizability for C1to C4

Dye	β_{max}^{a} $\times(10^{-30}$ esu)	β_{CT}^{b} $\times (10^{-30}$ esu)	β_0^{c} $\times (10^{-30}$ esu)	γ_{min}^{d} $\times (10^{-36}$ esu)	γ_{max}^{d} $\times (10^{-36}$ esu)	γ_{SD}^{e} $\times (10^{-36}$ esu)	γ^{f} $\times (10^{-36}$ esu)
C1	6151	38	255	−18309	32237	32	813
C2	10,860	22	259	−41244	164977	26	1286
C3	5879	45	306	−17439	69757	48	917
C4	10,551	38	316	−39573	158293	38	1412

Table 5 Two-photon absorption cross-section of C1 to C4

Solvent	C1	C2	C3	C4
Toluene	115	15	106	54
DCM	158	38	133	39
EtOAc	91	36	91	26
Dioxane	73	22	144	30
EtOH	81	16	85	71
MeOH	50	9	155	65
ACN	121	15	72	60
DMF	157	–	170	–
DMSO	172	–	146	–

*The two-photon absorption cross section $\boldsymbol{\sigma_2(\nu)}$ in GM units where 1 GM = 10^{-50} photons cm^{-4} s^{-1}

$$\sigma_2(\nu) = \frac{12}{5}\ \frac{\ln 10\ \pi 10^3 L^4}{N_A h c^2 n^2}\left(\frac{\epsilon_{10(\nu)}}{\bar{v}_{10}}\right).\Delta\mu_{10}^2 \tag{7}$$

where L is the Lorentzian local field factor $L = \left(\frac{2n^2+2}{3}\right)$, $\epsilon_{10(\nu)}$ is molar extrinction coefficient, $\bar{v}_{10}$ is emission frequency in wavenumber (cm^{-1}), $\Delta\mu_{10}$ is transition dipole moment obtained from spectral shift measurements, h is the Planck's constant, c is the speed of light, n is the refractive index, and N_A is Avogadro's number.

Dyes **C2 and C4** show the lowest TPA cross-section below 100 GM, while **C1**and **C3** dyes show above 100 GM Table 5.

Conclusion

In this paper, we present a critical evaluation of the diverse computational approaches based on DFT and TD-DFT methods using various GH and RSH functionals and the basis function 6–311 + G(d, for evaluating NLO parameters. The GHs overestimate α_0 and β_0 values. The RSHs functionals wB97, wB97-X and HISSbPBE, HSEH1PBE give comparable β_0 and γ_0 values respectively and the parameters are in good agreement with each other. An intensification in the acceptor strength in coumarin augments charge transfer features and escalates NLO response. It is clear that parameters are linked to electron delocalization ensuing from electron accepting strength of the cyano group. Furthermore, this relation can be also seen in results obtained with computations using different hybrid DFT functionals. In MAE calculations of GH and RSH functionals, large significant differences in values are not observed. Coumarin dyes display significant molecular second and third non linearity than urea and can provide the basis for future design of effective NLO materials.

Acknowledgements One of the authors SK is thankful to UGC for granting study leave (FIP) and SIES College for approving the study leave.

Publisher's note Springer Nature remains neutral with regard to jurisdictional claims in published maps and institutional affiliations.

References

1. Dalton LR, Benight SJ, Johnson LE, Knorr DB, Kosilkin I, Eichinger BE, Robinson BH, Jen AK (2011) Systematic Nanoengineering of soft matter organic. Chem Mater 23:430–445. https://doi.org/10.1021/cm102166j
2. Dalton LR, Sullivan P a, Bale DH (2010) Electric field poled organic electro-optic materials: state of the art and future prospects. Chem Rev 110:25–55. https://doi.org/10.1021/cr9000429
3. Lupo D (1995) Molecular nonlinear optics: materials, physics, and devices. Edited byJ. Zyss, academic press, San Diego. CA 1994, XIII, 478 pp., hardcover, ISBN 0-12-784450-3. Adv Mater 7:248–249. https://doi.org/10.1002/adma.19950070232
4. Frenette M, Hatamimoslehabadi M, Bellinger-Buckley S, Laoui S, Bag S, Dantiste O, Rochford J, Yelleswarapu C (2014) Nonlinear optical properties of multipyrrole dyes. Chem Phys Lett 608:303–307. https://doi.org/10.1016/j.cplett.2014.06.002
5. Liu X, Wang D, Gao H, Yang Z, Xing Y, Cao H, He W, Wang H, Gu J, Hu H (2016) Nonlinear optical properties of symmetrical and asymmetrical porphyrin derivatives with click chemistry modification. Dyes Pigments 134:155–163. https://doi.org/10.1016/j.dyepig.2016.07.010
6. Song W, He C, Zhang W, Gao Y, Yang Y, Wu Y, Chen Z, Li X, Dong Y (2014) Synthesis and nonlinear optical properties of reduced graphene oxide hybrid material covalently functionalized with zinc phthalocyanine. Carbon N Y 77:1020–1030. https://doi.org/10.1016/j.carbon.2014.06.018
7. Chen Z, Dong S, Zhong C, Zhang Z, Niu L, Li Z, Zhang F (2009) Photoswitching of the third-order nonlinear optical properties of azobenzene-containing phthalocyanines based on reversible host–guest interactions. J Photochem Photobiol A Chem 206:213–219. https://doi.org/10.1016/j.jphotochem.2009.07.005
8. Song W, Xiao X, He C, Mao G, Gao Y, Chen Z, Dong Y, Wu Y (2016) Electrostatic self-assembled design strategy for tetracarboxylic Nickel (II) naphthalocyanine ultrathin film for high-performance nonlinear optical properties. Opt. Mater. (Amst). 60(6–12):6–12. https://doi.org/10.1016/j.optmat.2016.07.002
9. Ashraf M, Teshome A, Kay AJ, Gainsford GJ, Bhuiyan MDH, Asselberghs I, Clays K (2013) NLO chromophores containing dihydrobenzothiazolylidene and dihydroquinolinylidene donors with an azo linker: synthesis and optical properties. Dyes Pigments 98:82–92. https://doi.org/10.1016/j.dyepig.2013.01.010
10. Castro MCR, Schellenberg P, Belsley M, Fonseca AMC, Fernandes SSM, Raposo MMM (2012) Design, synthesis and evaluation of redox, second order nonlinear optical properties and theoretical DFT studies of novel bithiophene azo dyes functionalized with thiadiazole acceptor groups. Dyes Pigments 95:392–399. https://doi.org/10.1016/j.dyepig.2012.05.014
11. Tathe AB, Gupta VD, Sekar N (2015) Synthesis and combined experimental and computational investigations on spectroscopic and photophysical properties of red emitting 3-styryl coumarins. Dyes Pigments 119:49–55. https://doi.org/10.1016/j.dyepig.2015.03.023
12. Tathe AB, Sekar N (2016) Red emitting Coumarin—azo dyes : synthesis, characterization, linear and non-linear optical

properties-experimental and computational approach. J Fluoresc 26:1279–1293. https://doi.org/10.1007/s10895-016-1815-2
13. Chemate S, Sekar N (2016) Indole-based NLOphoric donor-π-acceptor Styryl dyes: synthesis, spectral properties and computational studies. J Fluoresc 26:2063–2077. https://doi.org/10.1007/s10895-016-1901-5
14. Zhu M, Jiang L, Yuan M, Liu X, Ouyang C, Zheng H, Yin X, Zuo Z, Liu H, Li Y (2008) Efficient tuning nonlinear optical properties: synthesis and characterization of a series of novel poly (aryleneethynylene) s co-containing BODIPY. J Polym Sci Part A Polym Chem 46:7401–7410. https://doi.org/10.1002/pola.23045
15. Ulrich G, Barsella A, Boeglin A, Niu S, Ziessel R (2014) BODIPY-bridged push-pull chromophores for nonlinear optical applications. ChemPhysChem 15:2693–2700. https://doi.org/10.1002/cphc.201402123
16. Telore RD, Jadhav AG, Sekar N (2016) NLOphoric and solid state emissive BODIPY dyes containing N -phenylcarbazole core at meso position – synthesis, photophysical properties of and DFT studies. J Lumin 179:420–428. https://doi.org/10.1016/j.jlumin.2016.07.035
17. Thakare SS, Sreenath MC, Chitrambalam S, Joe IH, Sekar N (2017) Non-linear optical study of BODIPY-benzimidazole conjugate by solvatochromic, Z-scan and theoretical methods. Opt Mater (Amst) 64:453–460. https://doi.org/10.1016/j.optmat.2017.01.020
18. McGoverin CM, Walsh TJ, Gordon KG, Kay AJ, Woolhouse AD (2007) Predicting nonlinear optical properties in push–pull molecules based on methyl pyridinium donor and 3-cyano-5,5-dimethyl-2(5H)-furanylidene-propanedinitrile acceptor units using vibrational spectroscopy and density functional theory. Chem Phys Lett 443:298–303. https://doi.org/10.1016/j.cplett.2007.06.068
19. Reish ME, Kay AJ, Teshome A, Asselberghs I, Clays KL, Gordon KC (2012) Testing computational models of Hyperpolarizability in a Merocyanine dye using spectroscopic and DFT methods. J Phys Chem A 116:5453–5463. https://doi.org/10.1021/jp301455r
20. Barnsley JE, Shillito GE, Larsen CB, Salm HV, Wang LE, Lucas NT (2016) Gordon, K/G.: benzo [c][1,2,5] thiadiazole donor−acceptor dyes: a synthetic, spectroscopic, and computational study. J Phys Chem A 120:1853−−1866. https://doi.org/10.1021/acs.jpca.6b00447
21. Dreuw A, Head-Gordon M (2005) Single-reference ab initio methods for the calculation of excited states of large molecules. Chem Rev 105:4009–4037. https://doi.org/10.1021/cr0505627
22. Andzelm J, Rawlett A, Dougherty J, Govind N, Baer R (2008) Performance of DFT methods in the calculation of optical spectra of chromophores. 2008 Proc. Dep. Def. High perform. Comput. Mod. Progr. Users Gr. Conf - Solving Hard Probl 235–240. https://doi.org/10.1109/DoD.HPCMP.UGC.2008.80
23. Tozer, D.J., Amos, R.D., Handy, N.C., Roos, B.O., Serrano-ANDRES, L.: Does density functional theory contribute to the understanding of excited states of unsaturated organic compounds? Mol Phys 97, 859–868 (1999). doi:https://doi.org/10.1080/00268979909482888
24. Becke AD (1993) Density-functional thermochemistry. III. The role of exact exchange. J Chem Phys 98:5648–5652. https://doi.org/10.1063/1.464913
25. Wu Q, Ayers PW, Yang W (2003) Density-functional theory calculations with correct long-range potentials. J Chem Phys 119:2978–2990. https://doi.org/10.1063/1.1590631
26. Tozer DJ, Handy NC (1998) Improving virtual Kohn-sham orbitals and eigenvalues: application to excitation energies and static polarizabilities. J Chem Phys 109:10180–10189. https://doi.org/10.1063/1.477711
27. Van Leeuwen R, Baerends EJ (1994) Exchange-correlation potential with correct asymptotic behavior. Phys Rev A 49:2421–2431. https://doi.org/10.1103/PhysRevA.49.2421
28. Kirtman B, Lacivita V, Dovesi R, Reis H (2011) Electric field polarization in conventional density functional theory: from quasilinear to two-dimensional and three-dimensional extended systems. J Chem Phys 135(15401):154101. https://doi.org/10.1063/1.3649945
29. Loboda O, Zales R, Avramopoulos A, Luis J, Kirtman B, Tagmatarchis N (2009) Linear and nonlinear optical properties of [60] fullerene derivatives. J Phys Chem A 113:1159–1170. https://doi.org/10.1021/jp808234x
30. Van Faassen M, De Boeij PL, Van Leeuwen R, Berger JA, Snijders JG (2003) Application of time-dependent current-density-functional theory to nonlocal exchange-correlation effects in polymers. J Chem Phys 118:1044–1053. https://doi.org/10.1063/1.1529679
31. Champagne B, Perpète EA, Jacquemin D, van Gisbergen SJA, Baerends E-J, Soubra-Ghaoui C, Robins KA, Kirtman B (2000) Assessment of conventional density functional schemes for computing the dipole moment and (hyper) polarizabilities of push−pull π-conjugated systems †. J Phys Chem A 104:4755–4763. https://doi.org/10.1021/jp993839d
32. Champagne B, Perpète EA, Van Gisbergen SJA, Baerends EJ, Snijders JG, Soubra-Ghaoui C, Robins KA, Kirtman B (1998) Assessment of conventional density functional schemes for computing the polarizabilities and hyperpolarizabilities of conjugated oligomers: an ab initio investigation of polyacetylene chains. J Chem Phys 109:10489–10498. https://doi.org/10.1063/1.477731
33. Chakrabarti S, Ruud K (2009) Large two-photon absorption cross section: molecular tweezer as a new promising class of compounds for nonlinear optics. Phys Chem Chem Phys 11:2592–2596. https://doi.org/10.1039/b822395e
34. Ramakrishna G, Goodson T (2007) Excited-state deactivation of branched two-photon absorbing chromophores: a femtosecond transient absorption investigation. J Phys Chem A 111:993–1000. https://doi.org/10.1021/jp064004n
35. Kanis DR, Ratner MA, Marks TJ (1994) Design and construction of molecular assemblies with large second-order optical nonlinearities. Quantum chemical aspects. Chem Rev 94:195–242. https://doi.org/10.1021/cr00025a007
36. Garza AJ, Osman OI, Wazzan NA, Khan SB, Asiri AM, Scuseria GE (2014) A computational study of the nonlinear optical properties of carbazole derivatives: theory refines experiment. Theor Chem Accounts 133(1–8). https://doi.org/10.1007/s00214-014-1458-9
37. Jacquemin D, Perpte EA, Vydrov OA, Scuseria GE, Adamo C (2007) Assessment of long-range corrected functionals performance for n→ π* transitions in organic dyes. J Chem Phys 127(94102):094102. https://doi.org/10.1063/1.2770700
38. Vydrov O a, Heyd J, Krukau AV, Scuseria GE (2006) Importance of short-range versus long-range Hartree-Fock exchange for the performance of hybrid density functionals. J Chem Phys 125(74106):074106. https://doi.org/10.1063/1.2244560
39. Vydrov O a, Scuseria GE (2006) Assessment of a long-range corrected hybrid functional. J Chem Phys 125:234109. https://doi.org/10.1063/1.2409292
40. Yanai T, Tew DP, Handy NC (2004) A new hybrid exchange – correlation functional using the. Chem Phys Lett 393:51–57. https://doi.org/10.1016/j.cplett.2004.06.011
41. Iikura H, Tsuneda T, Yanai T, Hirao K (2001) A long-range correction scheme for generalized-gradient-approximation exchange functionals. J Chem Phys 115:3540–3544. https://doi.org/10.1063/1.1383587
42. Savin A, Flad H-J (1995) Density functionals for the Yukawa electron-electron interaction. Int J Quantum Chem 56:327–332. https://doi.org/10.1002/qua.560560417
43. Garza AJ, Scuseria GE, Khan SB, Asiri AM (2013) Assessment of long-range corrected functionals for the prediction of non-linear

optical properties of organic materials. Chem Phys Lett 575:122–125. https://doi.org/10.1016/j.cplett.2013.04.081
44. Nguyen KA, Rogers JE, Slagle JE, Day PN, Kannan R, Tan L-S, Fleitz PA, Pachter R (2006) Effects of conjugation in length and dimension on spectroscopic properties of Fluorene-based chromophores from experiment and theory. J Phys Chem A 110:13172–13182. https://doi.org/10.1021/jp0642645
45. Jacquemin D, Perpète EA, Medved M, Scalmani G, Frisch MJ, Kobayashi R, Adamo C (2007) First hyperpolarizability of polymethineimine with long-range corrected functionals. J Chem Phys 126(1–5). https://doi.org/10.1063/1.2741246
46. de Wergifosse M, Champagne B (2011) Electron correlation effects on the first hyperpolarizability of push–pull π-conjugated systems. J Chem Phys 134(74113). https://doi.org/10.1063/1.3549814
47. Zaleśny R, Bulik IW, Bartkowiak W, Luis JM, Avramopoulos A, Papadopoulos MG, Krawczyk P (2010) Electronic and vibrational contributions to first hyperpolarizability of donor-acceptor-substituted azobenzene. J Chem Phys 133:244308. https://doi.org/10.1063/1.3516209
48. Jacquemin D, Perpète EA, Scuseria GE, Ciofini I, Adamo C (2008) TD-DFT performance for the visible absorption spectra of organic dyes: conventional versus long-range hybrids. J Chem Theory Comput 4:123–135. https://doi.org/10.1021/ct700187z
49. Perpète EA, Jacquemin D, Adamo C, Scuseria GE (2008) Revisiting the nonlinear optical properties of polybutatriene and polydiacetylene with density functional theory. Chem Phys Lett 456:101–104. https://doi.org/10.1016/j.cplett.2008.02.086
50. Jacquemin D, Perpète EA, Scuseria GE, Ciofini I, Adamo C (2008) Extensive TD-DFT investigation of the first electronic transition in substituted azobenzenes. Chem Phys Lett 465:226–229. https://doi.org/10.1016/j.cplett.2008.09.071
51. Song JW, Watson MA, Sekino H, Hirao K (2008) Nonlinear optical property calculations of polyynes with long-range corrected hybrid exchange-correlation functionals. J Chem Phys 129(24117). https://doi.org/10.1063/1.2936830
52. Kamiya M, Sekino H, Tsuneda T, Hirao K (2005) Nonlinear optical property calculations by the long-range-corrected coupled-perturbed Kohn-sham method. J Chem Phys 122:234111. https://doi.org/10.1063/1.1935514
53. Tawada Y, Tsuneda T, Yanagisawa S, Yanai T, Hirao K, Tawada Y, Tsuneda T, Yanagisawa S (2004) A long-range-corrected time-dependent density functional theory. J Chern Phys 120:8425. https://doi.org/10.1063/1.1688752
54. Nakano M, Champagne B (2016) Nonlinear optical properties in open-shell molecular systems. WIREs Comput Mol Sci 6:198–210. https://doi.org/10.1002/wcms.1242
55. Smith MB, Michl J (2010) Singlet fission. Chem Rev 110:6891–6936. https://doi.org/10.1021/cr1002613
56. Frisch MJ, Trucks GW, Schlegel HB, Scuseria GE, Robb MA, Cheeseman JR, Scalmani G, Barone V, Mennucci B, Petersson GA, Nakatsuji HCM, Li X, Hratchian HP, Izmaylov AF, Bloino J, Zheng G, Sonnenberg JL, Hada M, Ehara M, Toyota K, Fukuda R, Hasegawa J, Ishida M, Nakajima T, Honda Y, Kitao O, Nakai H, Vreven T, Montgomery JA, Jr; Peralta JE, Ogliaro F, Bearpark M, Heyd JJ, Brothers E, Kudin KN, Staroverov VN, Kobayashi R, Normand J, Raghavachari K, Rendell A, Burant JC, Iyengar SS, Tomasi J, Cossi M, Rega N, Millam N J, Klene M, Knox J E, Cross JBB V, Adamo C, Jaramillo J, Gomperts R, Stratmann RE, Yazyev O, Austin AJ, Cammi R, Pomelli C, Ochterski JW, Martin RL, Morokuma K, Zakrzewski VG, Voth GA, Salvador P, Dannenberg J J, Dapprich S, Daniels AD, Farkas O, Foresman JB, Ortiz JV, Cioslowski, J, Fox DJ: Gaussian 09, Revision C01, (2010)
57. Dooley R, Milfeld K, Guiang C, Pamidighantam S, Allen G (2005) Computational chemistry grid production cyberinfrastructure for computational chemistry, proc. 13th Annu. Mardi Gras Conf. Bat. Rouge, LA 83
58. Dooley, R., Milfeld, K., Guiang, C., Pamidighantam, S., G. Allen (2005) Cluster computing through an application-oriented computational chemistry grid, proc. 2005 Linux Clust. HPC Revolut
59. Dooley R, Milfeld K, Guiang C, Pamidighantam S, Allen G (2006) From proposal to production: lessons learned developing the computational chemistry grid cyberinfrastructure. J Grid Comput 4:195–208. https://doi.org/10.1007/s10723-006-9043-7
60. Lee C, Yang W, Parr RG (1988) Development of the Colle-Salvetti correlation-energy formula into a functional of the electron density. Phys Rev B 37:785–789. https://doi.org/10.1103/PhysRevB.37.785
61. Petersson GA, Bennett A, Tensfeldt TG, Allaham MA, Shirley WA, Petersson GA, Bennett A, Tensfeldt TG, Ai-laham MA, Shirley WA (1988) A complete basis set model chemistry . I . The total energies of closedshell atoms and hydrides of the firstrow elements A complete basis set model chemistry. I. The total energies of closed-shell atoms and hydrides of the first-row elements. J Chern Phys 89:2193. https://doi.org/10.1063/1.455064
62. Zhao Y, Truhlar DG (2008) The M06 suite of density functionals for main group thermochemistry , thermochemical kinetics , noncovalent interactions , excited states , and transition elements : two new functionals and systematic testing of four M06-class functionals and 12 other fun. Theor Chem Accounts 120:215–241. https://doi.org/10.1007/s00214-007-0310-x
63. Runge E, Gross EKU (1984) Density-functional theory for time-dependent systems. Phys Rev Lett 52:997–1000. https://doi.org/10.1103/PhysRevLett.52.997
64. Tomasi J, Mennucci B, Cammi R (2005) Quantum mechanical continuum solvation models. Chem Rev 105:2999–3093. https://doi.org/10.1021/cr9904009
65. Vidya S, Ravikumar C, Hubert Joe I, Kumaradhas P, Devipriya B, Raju K (2011) Vibrational spectra and structural studies of nonlinear optical crystal ammonium D, L-tartrate: a density functional theoretical approach. J Raman Spectrosc 42:676–684. https://doi.org/10.1002/jrs.2743
66. Geerlings P, De Proft F, Langenaeker W (2003) Conceptual density functional theory. Chem Rev 103:1793–1874. https://doi.org/10.1021/cr990029p
67. Hehre WJ, Ditchfield R, Pople J a (1972) Self—consistent molecular orbital methods. XII. Further extensions of Gaussian—type basis sets for use in molecular orbital studies of organic molecules. J Chem Phys 56:2257–2261. https://doi.org/10.1063/1.1677527
68. Avci D, Tamer Ö, Atalay Y (2016) Solvatochromic effect on UV-vis absorption and fluorescence emission spectra, second- and third-order nonlinear optical properties of dicyanovinyl-substituted thienylpyrroles: DFT and TDDFT study. J Mol Liq 220:495–503. https://doi.org/10.1016/j.molliq.2016.05.023
69. Johnson LE, Dalton LR, Robinson BH (2014) Optimizing calculations of electronic excitations and relative hyperpolarizabilities of electrooptic chromophores. Acc Chem Res 47:3258–3265. https://doi.org/10.1021/ar5000727
70. Castet F, Rodriguez V, Pozzo J-L, Ducasse L, Plaquet A, Champagne B (2013) Design and characterization of molecular nonlinear optical switches. Acc Chem Res 46:2656–2665. https://doi.org/10.1021/ar4000955
71. Swart M, Snijders JG, Th P, Duijnen V (2004) Polarizabilities of amino acid residues. J Comput methods Sci Eng 4:419–425
72. Solomon RV, Veerapandian P, Vedha SA, Venuvanalingam P (2012) Tuning nonlinear optical and optoelectronic properties of vinyl coupled triazene chromophores: a density functional theory and time-dependent density functional theory investigation. J Phys Chem A 116:4667–4677. https://doi.org/10.1021/jp302276w
73. Vargas J, Springborg M, Kirtman B (2014) Electronic responses of long chains to electrostatic fields: Hartree-Fock vs. density-

functional theory: a model study. J Chem Phys 140:054117. https://doi.org/10.1063/1.4864038
74. Thanthiriwatte KS, Nalin de Silva K (2002) Non-linear optical properties of novel fluorenyl derivatives—ab initio quantum chemical calculations. J Mol Struct THEOCHEM 617:169–175. https://doi.org/10.1016/S0166-1280(02)00419-0
75. Asiri AM, Khan SA, Al-Amoudi MS, Alamry KA (2012) Synthesis, characterization, absorbance, fluorescence and non linear optical properties of some donor acceptor chromophores. Bull Kor Chem Soc 33:1900–1906. https://doi.org/10.5012/bkcs.2012.33.6.1900
76. Tathe AB, Sekar N (2016) Red emitting NLOphoric 3-styryl coumarins : experimental and computational studies. Opt. Mater. (Amst). 51:121–127. https://doi.org/10.1016/j.optmat.2015.11.031
77. Arivazhagan M, Kavitha R, Subhasini VP (2014) Spectrochimica Acta part a : molecular and biomolecular spectroscopy conformational analysis , UV – VIS , MESP , NLO and NMR studies. Spectrochim ACTA PART A Mol Biomol Spectrosc 128:701–710. https://doi.org/10.1016/j.saa.2014.02.102
78. Chaitanya K, Ju XH, Heron BM, Gabbutt CD (2013) Vibrational spectra and static vibrational contribution to first hyperpolarizability of naphthopyrans—a combined experimental and DFT study. Vib Spectrosc 69:65–83. https://doi.org/10.1016/j.vibspec.2013.09.010
79. Robert WG, Zale R, Lipkowski P, Bartkowiak W, Reis H, Papadopoulos MG, Luis JM, Kirtman B (2011) Electronic structure , bonding , spectra , and linear and nonlinear electric properties of Ti @ C 28. J Phys Chem A 115:10370–10381. https://doi.org/10.1021/jp206331n
80. Zaleśny R, Wójcik G, Mossakowska I, Bartkowiak W, Avramopoulos A, Papadopoulos MG (2009) Static electronic and vibrational first hyperpolarizability of meta-dinitrobenzene as studied by quantum chemical calculations. J Mol Struct THEOCHEM 907:46–50. https://doi.org/10.1016/j.theochem.2009.04.011
81. Kuzyk MG (2006) Fundamental limits of all nonlinear-optical phenomena that are representable by a second-order nonlinear susceptibility. J Chem Phys 125:1–11. https://doi.org/10.1063/1.2358973
82. Pérez-Moreno J, Zhao Y, Clays K, Kuzyk MG (2007) Modulated conjugation as a means for attaining a record high intrinsic hyperpolarizability. Opt Lett 32:59–61. https://doi.org/10.1364/OL.32.000059
83. Kuzyk MG (2000) Fundamental limits on third-order molecular susceptibilities. Opt Lett 25:1183–1185. https://doi.org/10.1364/OL.25.001183
84. Kuzyk MG (2000) Physical limits on electronic nonlinear molecular susceptibilities. Phys Rev Lett 85:1218–1221. https://doi.org/10.1103/PhysRevLett.85.1218
85. Kogej T, Beljonne D, Meyers F, Perry JW, Marder SR, Brédas JL (1998) Mechanisms for enhancement of two-photon absorption in donor–acceptor conjugated chromophores. Chem Phys Lett 298:1–6. https://doi.org/10.1016/S0009-2614(98)01196-8
86. Drobizhev M, Meng F, Rebane A, Stepanenko Y, Nickel E, Spangler CW (2006) Strong two-photon absorption in new asymmetrically substituted porphyrins: interference between charge-transfer and intermediate-resonance pathways. J Phys Chem B 110:9802–9814. https://doi.org/10.1021/jp0551770
87. Rodrigues CAB, Mariz IFA, Maçôas EMS, Afonso CAM, Martinho JMG (2012) Two-photon absorption properties of push–pull oxazolones derivatives. Dyes Pigments 95:713–722. https://doi.org/10.1016/j.dyepig.2012.06.005